Supergene alteration of a refractory epithermal gold mineralization: The Perama Hill deposit, NE Greece

Triantafyllidis S.[1], Skarpelis N.[2]

[1]School of Mining and Metallurgical Engineering, Section of Geologic Sciences, National Technical University of Athens, 9 Iroon Polytechneiou str., 157 80, Zografou, Athens, Greece

[2]Faculty of Geology and Geoenvironment, Panepistimiopoli 157 84, Zografou, Athens, Greece

Tel.: 210-7724468, email: striantafyllidis@metal.ntua.gr

Abstract

Supergene alteration phenomena have affected the upper part of the Perama Hill epithermal mineralization hosted in the felsic sandstone (oxide sector). The very low acid buffering capacity of the porous sandstone combined with the disseminated character of pyrite and sulfosalts, resulted in extensive weathering. Goethite and hematite predominate in the upper part of the mineralized sandstone revealing pervasive oxidation and leaching of heavy metals. A transitional zone to the refractory sulfide mineralization is detected close to the underlying andesitic breccia. Free Au grains are identified in the upper, oxide sector of the deposit, with the highest Au grades being observed at the upper and lower part of the sandstone, the latter located close to the transition zone with the underlying andesitic breccia. Acid rock drainage identified in both surface and ground water samples in the vicinity of the Perama Hill epithermal deposit indicates active oxidation of the sulfide sector of the deposit.

Key words: *Intermediate sulfidation, disseminated ore, oxidation, native Au*

Περίληψη

Το κοίτασμα χρυσού του λόφου του Περάματος βρίσκεται περίπου 30 χλμ δυτικά-βορειοδυτικά της πόλης της Αλεξανδρούπολης και εντοπίζεται κατά μήκος μιας ΒΒΑ διεύθυνσης ρηξιγενούς ζώνης που καθορίζει το βορειοανατολικό όριο της τάφρου των Πετρωτών και η οποία φέρνει σε επαφή τους Καινοζωικούς ηφαιστειο-ιζηματογενείς σχηματισμούς της λεκάνης της Μαρώνειας με Μεσοζωικής ηλικίας μεταμορφωμένα πετρώματα της Περιροδοπικής. Το κοίτασμα φιλοξενείται σε ψαμμίτες που υπέρκεινται μιας ακολουθίας ανδεσιτικών λατυποπαγών, έχει σχήμα μανιταριού και εκτείνεται σε μήκος 750 m σε διεύθυνση Β-Ν και 300 m σε διεύθυνση Α-Δ. Το πάχος του κοιτάσματος κυμαίνεται από 15 έως 20 m στα άκρα, ενώ στο κέντρο φθάνει σε πάχος τα 125 m. Η μεταλλοφορία που φιλοξενείται στα ανδεσιτικά λατυποπαγή βρίσκεται υπό τεκτονικό έλεγχο, ενώ στον υπερκείμενο ψαμμίτη είναι κυρίως διάσπαρτη. Σκοπός της παρούσας έρευνας είναι η μελέτη της επίδρασης των φαινομένων υπεργενετικής αλλοίωσης στην επιθερμική μεταλλοφορία και η αναγνώριση των φυσικοχημικών συνθηκών που επικρά-

---

ΥΠΕΡΓΕΝΕΤΙΚΗ ΑΛΛΟΙΩΣΗ ΔΥΣΚΑΤΕΡΓΑΣΤΗΣ ΕΠΙΘΕΡΜΙΚΗΣ ΜΕΤΑΛΛΟΦΟΡΙΑΣ ΧΡΥΣΟΥ: ΚΟΙΤΑΣΜΑ ΛΟΦΟΥ ΠΕΡΑΜΑΤΟΣ, ΒΑ ΕΛΛΑΔΑ

Τριανταφυλίδης Σ., Σκαρπέλης Ν.

τησαν κατά την οξείδωσή της και τελικά στο σχηματισμό κόκκων ελεύθερου χρυσού. Συλλέχθηκαν δείγματα πυρήνων από 15 γεωτρήσεις κατά μήκος του άξονα Β-Ν του κοιτάσματος, μέχρι βάθους 262 m από την επιφάνεια. Τα δείγματα μελετήθηκαν με Ηλεκτρονικό Μικροσκόπιο Σάρωσης με Ανιχνευτή Διασποράς Ενέργειας, με Περιθλασιμετρία Ακτίνων-Χ και Οπτική Μικροσκοπία, για την αναγνώριση των υπογενετικών και υπεργενετικών ορυκτολογικών φάσεων. Ταυτόχρονα, γειτονικά του κοιτάσματος συλλέχθηκαν δείγματα επιφανειακών (ρέμματα) και υπεδαφικών υδάτων (πηγάδια) για μελέτη πιθανής επίδρασης σύγχρονων φαινομένων υπεργενετικής αλλοίωσης και υποβάθμισης της ποιότητας των απορρεόντων υδάτων. Τα αποτελέσματα των ορυκτολογικών και ιστολογικών μελετών έδειξαν ότι η ζώνη οξείδωσης του κοιτάσματος του λόφου του Περάματος ακολουθεί περίπου το όριο μεταξύ των υποκείμενων ανδεσιτικών λατυποπαγών και του υπερκείμενου ψαμμίτη. Στο κέντρο φθάνει σε βάθος περίπου 100 m από την επιφάνεια, ενώ στα άκρα κυμαίνεται μεταξύ 20 και 25 m. Η μελέτη δειγμάτων πυρήνων γεωτρήσεων από τον υπερκείμενο ψαμμίτη απέδειξε την παρουσία κόκκων ελεύθερου χρυσού με κυμαινόμενο περιεχόμενο σε άργυρο (1 έως και 3% κ.β.) και μέγεθος μεταξύ 1 και 10 μm. Οι υψηλότερες συγκεντρώσεις κόκκων χρυσού εντοπίζονται στο ανώτερο τμήμα του ψαμμίτη κοντά στην επιφάνεια και στο κατώτερο κοντά στη ζώνη μετάβασης με τα υποκείμενα ανδεσιτικά λατυποπαγή. Στο ανώτερο τμήμα της ζώνης οξείδωσης τα φαινόμενα υπεργενετικής αλλοίωσης είναι ιδιαίτερα έντονα. Τα μεταλλικά ορυκτά σιδηροπυρίτης και τενναντίτης είναι έντονα οξειδωμένα με κυριότερα τελικά προϊόντα τις δυσδιάλυτες φάσεις του Fe(III) γκαιτίτη και αιματίτη. Επίσης, το ανώτερο τμήμα της ζώνης οξείδωσης εμφανίζει έντονη έκπλυση βαρέων μετάλλων, όπως χαλκός και ψευδάργυρος. Ζώνες liesegang, ίχνη σιδηροπυρίτη και τενναντίτη, υψηλό φορτίο σε γκαιτίτη και αιματίτη ως εμποτισμοί με λεπτόκοκκο καολινίτη μεταξύ κλαστών χαλαζία και κόκκοι ελεύθερου χρυσού συνδεόμενοι με μάζες καολινίτη±γκαιτίτη αποτελούν τα πιο κοινά ιστολογικά χαρακτηριστικά του ανώτερου τμήματος της ζώνης οξείδωσης, το οποίο στο κέντρο του κοιτάσματος φθάνει σε βάθη μέχρι και 45 m από την επιφάνεια. Κάτω από το ανώτερο, έντονα οξειδωμένο τμήμα, τα φαινόμενα οξείδωσης είναι σχετικά περιορισμένα. Κατά θέσεις, τα πρωτογενή μεταλλικά ορυκτά παραμένουν υγιή. Γκαιτίτης και αιματίτης εντοπίζονται κατά μήκος ρωγμών και σπασιμάτων του πυριτιωμένου ψαμμίτη. Τοπικά παρατηρούνται ψευδομορφώσεις γκαιτίτη κατά σιδηροπυρίτη, ενώ σε άλλες περιπτώσεις ο σιδηροπυρίτης αντικαθίσταται περιφερειακά από αλλοτριόμορφο γιαροσίτη. Ορυκτολογική μελέτη δειγμάτων πυρήνων γεωτρήσεων κοντά στη ζώνη μετάβασης μεταξύ του υπερκείμενου ψαμμίτη και των υποκείμενων ανδεσιτικών λατυποπαγών αποκάλυψε την παρουσία κόκκων ελεύθερου χρυσού μεταξύ κλαστών χαλαζία. Από την άλλη πλευρά, φαινόμενα υπεργενετικής αλλοίωσης δεν παρατηρήθηκαν στη δυσκατέργαστη μεταλλοφορία που φιλοξενείται στα υποκείμενα ανδεσιτικά λατυποπαγή, ενώ επίσης δεν εντοπίζονται κόκκοι ελεύθερου χρυσού. Τα επιφανειακά και υποεπιφανειακά ύδατα που συλλέχθηκαν γειτονικά του κοιτάσματος χαρακτηρίζονται ως όξινα με υψηλό φορτίο βαρέων μετάλλων. Η χαμηλή ποιότητα των υδάτων είναι αποτέλεσμα των συνεχιζόμενων φαινομένων υπεργενετικής αλλοίωσης που δρουν ακόμη και σήμερα στη διάσπαρτη μεταλλοφορία που φιλοξενείται στον ψαμμίτη. Ελαφρά όξινα και οξειδωτικά ρευστά κατεισδύουν μεταξύ

των πόρων του ψαμμίτη και προσβάλλουν τη διάσπαρτη μεταλλοφορία, με τελικό αποτέλεσμα την πτώση της ποιότητας των υδάτων που αποστραγγίζουν τον ψαμμίτη του λόφου του Περάματος.
Λέξεις κλειδιά: *Ενδιάμεσης θείωσης, διάσπαρτη μεταλλοφορία, οξείδωση, ελεύθερος χρυσός*

1. Introduction

A significant number of epithermal systems occur in several parts of the Tertiary volcanosedimentary basin of Thrace, NE Greece. Exploration for gold is still carried out to this day, recognising the Tertiary Thrace basin as a Au-rich terrain (Skarpelis, et al., 1987; Michael et al., 1988; Michael et al., 1989; Michael et al., 1995; Bridges et al., 1997; Skarpelis, et al., 1999; Voudouris et al., 2003) due to favourable structures and magmatism. Several epithermal Au prospects were investigated during the last 15 years in the area with those of Perama and Sapes being the most important, verifying the Au potential of Thrace (Border et al., 1999; McAlister et al., 1999; Shaw and Constantinides, 2001; Lescuyer et al., 2003).

The aim of the present paper is to determine the effect of supergene alteration of the epithermal mineralization at Perama hill and to identify the physicochemical conditions that prevailed during supergene alteration which led to free Au formation.

2. Geological setting – ore deposit geology

The Perama Hill gold deposit is located 30 km west-northwest of the city of Alexandroupolis, Thrace, NE Greece (Fig. 1A). The topography of the region consists of low altitude hills, with height ranging between 250 and 300 m above sea level. Vegetation is sparse comprising mainly thorn and scrub bushes and oak trees, and the climate is characterized as Mediterranean with mean annual rainfall of 560 mm (Juras et al., 2010).

The Perama Hill epithermal system is controlled by a NNE trending fault zone that defines the northeastern border of the Petrota graben and brings in contact the Cenozoic volcano-sedimentary formation of the Maronia basin with strongly deformed and drag folded Mesozoic marbles, greenschists and calc-schists of the Circum-Rhodope Belt (Lescuyer et al., 2003) (Fig. 1B). Transtensional opening of the graben during Late Eocene-Oligocene facilitated intrusion of calc-alkaline to high-K calc-alkaline magma bodies (Eleftheriadis, 1990; Christofides et al, 1998) with formation of extrusive and shallow level intrusive volcanic suites. Pecskay et al. (2003) distinguished two main periods of volcanic activity in the region, an Oligocene (33.5 - 25.4 Ma) and a Lower Miocene (22.0 - 19.6 Ma), based on K/Ar ages obtained from whole rock (lavas and tuffs) and biotite separates. During Oligocene, sinistral strike-slip reactivation of basement faults and graben margins is considered synchronous with the hydrothermal activity that led to the formation of the mineralization (Lescuyer et al., 2003).

The deposit is hosted in felsic volcanic sandstone overlying a sequence of andesitic volcanic breccia. A volcanoclastic conglomerate unit with ranging thickness marks the transition be-

tween the two formations.
The sandstone is considered coeval with felsic eruptions at the western part of the graben and the presence of worm tubes and wood fragments indicate palustrine environment (Lescuyer et al., 2003).

The deposit is mushroom shaped and extends 750 m in a north-south direction and up to 300 m in an east-west direction with thickness varying from 15 m to 20 m at the borders and up to 125 m at the centre (Juras et al., 2010).

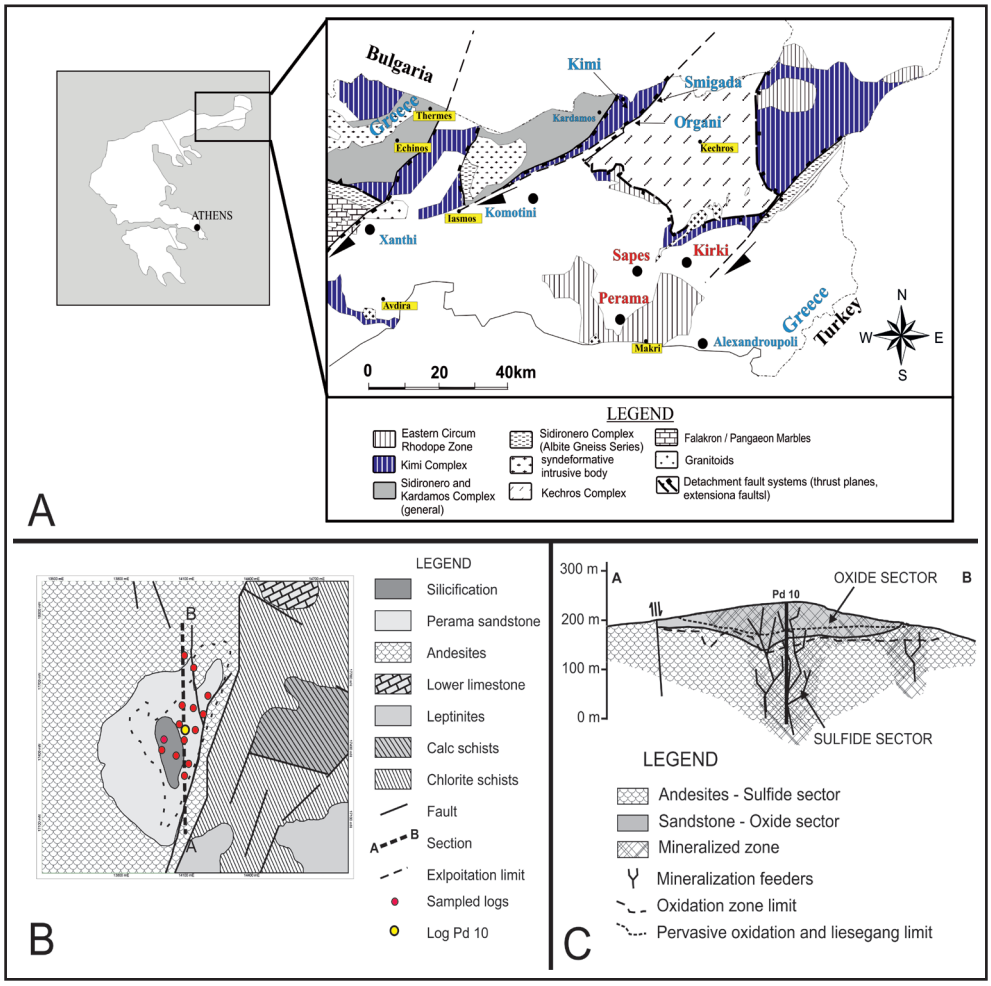

Fig. 1. *A. Simplified geological map of Eastern Macedonia – Thrace, NE Greece (after Krohe and Mposkos, 2002). B. Geological map of the Perama Hill deposit with locations of sampled logs (courtesy of Thracean Goldmining S.A. with modifications). C. Cross section (N-S direction) of the Perama Hill deposit indicating the limit of the oxidation zone (after Triantafyllidis, 2006 with modifications).*

Εικ. 1. *Α. Απλοποιημένος γεωλογικός χάρτης Ανατολικής Μακεδονίας – Θράκης, ΒΑ Ελλάδα (από Krohe και Mposkos, 2002). Β. Γεωλογικός χάρτης της περιοχής του κοιτάσματος του λόφου του Περάματος με τις θέσεις των γεωτρήσεων που δειγματίστηκαν (ευγενική παραχώρηση από την Thracean Goldmining S.A., με αλλαγές). C. Γεωλογική τομή διεύθυνσης Β-Ν από το κοίτασμα του λόφου του Περάματος, στην οποία εμφανίζεται το κατώτερο όριο της ζώνης οξείδωσης (από Triantafyllidis, 2006 με τροποποιήσεις).*

Hypogene mineralization is under tectonic control and occurs in distinct subvertical feeder zones, whereas in the overlying sandstone is mostly disseminated. The deposit is characterized as intermediate sulfidation (Skarpelis et al., 2006) or as high sulfidation overprinted by a later intermediate sulfidation stage (Voudouris et al., 2007).

Stable and radiogenic isotope data studies revealed the high to intermediate sulfidation character of the mineralization (Marschik et al., 2011). The deposit has been deeply oxidized and fine grained free gold mineralization is hosted in the sandstone (Skarpelis et al., 2006). Hence, two major sectors may be recognized in the Perama deposit: the upper, oxide sector with free gold which is the target for mineral exploitation by application of cyanide extraction technique, and the lower, sulfide sector. The calculated reserves (proven and probable) are 9.4 Mt with average grade 3.20 gr/tn Au and 3.75 gr/tn Ag. In the oxidized ore Au grades range between 5 and 10 g/tn whereas in the underlying sulfide sector Au grades are below 1 g/tn (Juras et al., 2010).

3. Sampling – Analytical methods

Drill core samples from 15 bore holes (Fig. 1B) along a N-S axis to depths down to 262 m were collected and used for the mineralogical investigation of both hypogene refractory mineralization and supergene mineral phases. Sampling was focused on those parts of drill cores where high in Au and base metals ore was detected, based on geochemical profiles and the grades provided by the company. A total number of 35 thin and polished sections were prepared, and a part from each sample was pulverized and homogenized for X-Ray diffraction. Mineral identification was carried out by combined optical microscopy, X-ray diffractometry and Scanning Electron Microscopy (SEM). X-ray diffractometry was carried out by using a SIEMENS D5005 X-ray diffractometer with Cu(kα) radiation at 40 kV/20 mA operating conditions. Scanning electron microscopy was performed using a Jeol JSM 5600 scanning electron microscope combined with energy dispersive X-ray spectrometry (OXFORD ISIS Link electron microprobe) and equipped with a Jeol Analytical back-scattered electron detector at the Laboratory of Economic Geology and Geochemistry, University of Athens. Operating conditions for the SEM were 20 kV accelerating voltage and 0.5 nA beam current. Counting time for each analysis was 50 sec, with 15 sec dead time. Several geochemical profiles of selected heavy metals of the studied boreholes were provided by courtesy of Thracean Gold Mining S.A. and used for the mineralogical and textural investigation (Fig. 2).

Stream and groundwater samples from the vicinity of the deposit were collected in order to investigate whether supergene alteration phenomena are active, affecting surface drainage and underground waters. Sampling was carried out in June and October 2003 applying standard sampling techniques. Water samples were commercially analyzed for cations contents. Concentrations of Fe, Mn, Cu, Pb, Zn, Cd, Ni, Co, As, Hg, and Sb were determined by an inductively coupled

plasma atomic emission spectrometer (ICP-AES). For Hg, the Hydride/ Cold vapor technique was applied in order to further lower the detection limit below 0.01 mg/L. Temperature, pH and Eh were measured on site while sulphate concentrations were measured at the Laboratory of Economic Geology and Geochemistry, University of Athens, by spectrophotometry (Hach DR 2000).

4. RESULTS

4.1. Hypogene mineralogy – Sulfide sector

Pyrite is the predominant sulfide mineral in the Perama Hill deposit with its concentrations increasing along with depth (Tabl. 1, Fig. 2). Pyrite is mostly disseminated and rarely forms patches and aggregates. Marcasite usually occurs in crystal sizes ranging between 5 and 10μm. Marcasite aggregates are observed along with pyrite. Tennantite and enargite participate in moderate proportions (Tables 1 and 2). Minor anglesite, sphalerite (mainly as inclusions in pyrite), Pb-sulfosalts and tellurides are identified as well. In the sulfide sector, Au-bearing phases include Au and Ag-Au tellurides in association with hessite and Ag-Bi tellurides. No primary silicates besides quartz are observed, indicating hydrothermal alteration and replacement by silica and to a lesser degree by kaolinite. Svanbergite-woodhouseite series phases are found in samples from both the oxide and the sulfide sector of the deposit (Tabl. 1). These phases are fine-grained forming aggregates and patches with kaolinite and euhedral unaltered pyrite and may indicate hypogene origin related to development of advance argillic alteration (Dill, 2001). Svanbergite-woodhouseite phases are members of the alunite – jarosite supergroup – APS with a general formula $AB_3(XO_4)_2(OH)_6$. The anion XO4-x is occupied either by S or P (Struntz and Tennyson, 1982; Scott, 1987; Jambor, 1999) with alunite being the most common phase. Late stage acidic fluids with increased P content may change alunite composition through coupled substitutions of $[K^+ + SO_4^{-2}]$ by $[(Ca,Sr)^{-2} + PO_4^{-3}]$ towards svanbergite-woodhouseite solid solutions (Dill, 2001). No supergene alteration is observed and primary sulfides and sulfosalts still remain (Fig. 3A).

Tabl. 1. Semiquantitative analyses of minerals identified by optical microscopy, X-ray diffraction and Scanning Electron Microscopy from drill core samples of the Perama hill Au deposit.

Sulfides, sulfosalts, native metals		Gangue		Supergene phases		Detrital phases in the sandstone	
Pyrite	+++++	Quartz	+++++	Goethite	+++	Rutile-anatase	++
Tennantite	++	K-feldspar	+	Hematite	+++	Zircon	+
Enargite	++	Kaolinite	+++	Jarosite	+	Monazite	+
Galena	+	Illite	+	Anglesite	+	Ilmenite	++
Sphalerite	+	Svanbergite-woodhouseite	+			Churchite	+
Pb-sulfosalts	+	Barite	++				
Marcasite	+						
Hessite	+						
Tetradymite	+						
Ag-Bi tellurides	+						
Au (±Ag) grains	+						

Tabl. 2. Representative chemical analyses of tennantite (out of 125) and enargite (out of 83) from the Perama Hill deposit (results in wt%).

	Tennantite		Enargite		
Mn	0.91	0.28	b.d.l.	b.d.l.	b.d.l.
Fe	4.19	7.02	0.27	0.27	2.97
Cu	39.52	36.19	46.11	45.93	43.81
Zn	5.24	6.19	b.d.l.	b.d.l.	b.d.l.
As	18.49	15.14	20.57	20.6	21.17
Sb	3.05	7.13	b.d.l.	b.d.l.	b.d.l.
S	27.15	27.99	31.19	31.07	32.18
TOTAL	**98.55**	**99.94**	**98.14**	**97.87**	**100.13**
Mn	0.25	0.08	-	-	-
Fe	1.14	1.89	0.02	0.02	0.21
Cu	9.43	8.56	2.94	2.93	2.72
Zn	1.22	1.42	-	-	-
As	3.74	3.04	1.11	1.12	1.11
Sb	0.38	0.88	-	-	-
S	12.84	13.12	3.93	3.93	3.96
TOTAL	**29**	**28.99**	**8**	**8**	**8**
Structural formulas calculated on the basis of 29 and 8 atoms for tennantite and enargite respectively					

Tabl. 3. Representative chemical analyses of jarosite (out of 65) from the Perama Hill deposit (results in wt%).

K_2O	Na_2O	Fe_2O_3	Al_2O_3	SO_3	TOTAL
9.05	0.45	37.7	7.6	33.1	87.9
9.20	0.22	44.30	2.83	32.5	89.1
8.12	1.05	45.47	2.40	32.89	89.9
A site		**B site**		**X site**	
0.93	0.07	2.28	0.72	2	
0.96	0.03	2.73	0.27	2	
0.84	0.16	2.77	0.23	2	
Compositions based on jarosite general formula $AB_3(XO_4)_2(OH)_6$ with XO_4 normalized to 2					

4.2. Supergene mineralogy – Oxide sector

The Au distribution and mineralogy of borehole Pd10 is shown in Fig. 2. The location of the borehole along with the large number of drill core samples studied (ranging in depth from 40 m to 262 m from the surface) provide a reliable profile on the distribution of hypogene and supergene phases identified in the ore, and insights on the geochemical environment prevailing during oxidation relative to depth.

Goethite and hematite are the predominant secondary phases identified in the oxidation zone (Tabl. 1, Fig. 2). Major textural forms in the oxide sector include patches of fine-grained goethite and hematite associated with fine-grained kaolinite between quartz clasts. Scarce pseudomorphs of goethite after euhedral pyrite are also identified at lower levels of the oxide sector with minor anglesite (after galena) and other secondary hydrous Fe-sulfates (Tabl. 1). Jarosite is identified in the lower level of the oxide sector and is usually enriched in Al with ranging Na content (Tabl. 3). Jarosite is closely associated with pyrite oxidation, forming anhedral grains around pyrite crystals. In the oxide sector, quartz is the predominant gangue mineral (Tabl. 1) appearing in two major forms.

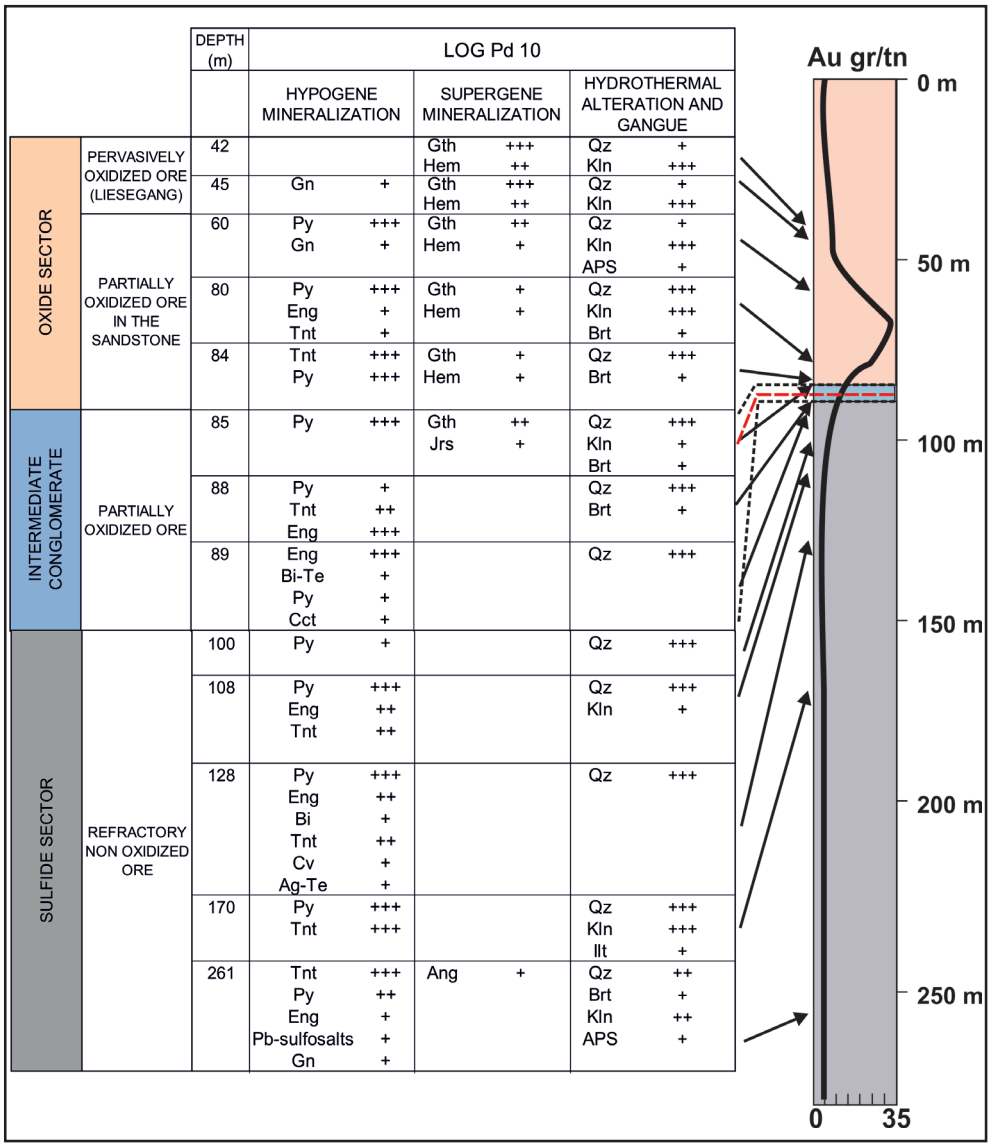

Fig. 2. *Lithological, mineralogical and geochemical fingerprint of borehole PD10 (after Skarpelis et al., 2006 with modifications). The Au distribution with depth was provided by courtesy of Thracean Gold Mining S.A. Abbreviations: Gn – galena, Py – pyrite, Eng – enargite, Tnt – tennantite, Bi-Te – Bi-tellurides, Bi – bismuth, Cv – covellite, Ag-Te – Ag-tellurides, Gth – goethite, Hem – hematite, Jrs – jarosite, Ang – anglesite, Qz – quartz, Kln – kaolinite, APS – Aluminum phosphates-sulfates, Brt – barite, Ilt – illite (after Whitney and Evans, 2010). (+++) major mineral constituents, (++) minor constituents, (+) subordinate constituents. Thick dashed red line indicates the limit of the oxidation zone.*

Εικ. 2. *Λιθολογικό, ορυκτολογικό και γεωχημικό προφίλ γεώτρησης Pd10 (από Skarpelis et al., 2006 με αλλαγές). Η κατανομή του Au σε βάθος παραχωρήθηκε ευγενικά από την Thracean Gold Mining S.A. Συντμήσεις ορυκτών: Gn – γαληνίτης, Py – σιδηροπυρίτης, Eng – εναργίτης, Tnt – τενναντίτης, Bi-Te – Bi-τελλουρίδια, Bi – βισμούθιο, Cv – κοβελίνης, Ag-Te – Ag-τελλουρίδια, Gth – γκαιτίτης, Hem – αιματίτης, Jrs – γιαροσίτης, Ang – αγκλεσίτης, Qz – χαλαζίας, Kln – καολινίτης, APS – φωσφορικά-θειικά αργιλίου, Brt – βαρίτης, Ilt – ιλλίτης (από Whitney και Evans, 2010). (+++) κύρια ορυκτολογικά συστατικά, (++) επουσιώδη, (+) σε ίχνη. Η κόκκινη διακεκομμένη γραμμή υποδεικνύει το όριο της ζώνης οξείδωσης.*

The first involves angular and subangular quartz and polycrystalline quartz clasts, while the second one includes fine-grained euhedral to subhedral quartz with its size ranging between 5 and 10 μm accompanied by fine-grained kaolinite and/or barite and is associated with hydrothermal alteration (silicification and argillic alteration). Kaolinite is the second most abundant gangue mineral after quartz. Aggregates of fine-grained crystals predominate, forming patches and filling voids between sandstone clasts and hydrothermal euhedral quartz. Minor pseudomorphs of kaolinite replacing detrital K-feldspar are also identified and limited to the upper part of the sandstone. Kaolinite pseudomorphs are also found at near-surface samples of the devitrified andesites at the northern part of the deposit. Further studies including oxygene isotope analyses on kaolinite samples from the oxide sector of the deposit are required to discriminate between hypogene and supergene origin. Illite is the second most abundant argillic phase after kaolinite. It is found mostly in the upper part of the overlying sandstone replacing micas, and in near-surface andesites replacing euhedral feldspars. Barite was identified in the majority of the analyzed samples. Barite crystals are euhedral to anhedral with size ranging from a few μm to several mm in length, and show typical characteristics of late stage deposition. Barite crystals are either found in quartz-barite veins and veinlets or as disseminations of large euhedral crystals between quartz clasts.

Tabl. 4. Physicochemical conditions and geochemical analyses of stream and underground water samples (sulfates and cation concentrations in mg/L, Eh in mV, conductivity – CND in μS/cm).

Sample	pH	Eh	CND	SO_4	As	Cd	Co	Cu	Fe	Mn	Ni	Pb	Zn
June 2003													
P1	3.2	227	3570	1700	bdl	bdl	0.283	0.012	8.8	10.4	0.16	bdl	0.7
October 2003													
P1	3.3	221	3530	2600	0.04	0.003	0.302	0.014	5.7	9.8	0.16	bdl	0.6
P2	4.1	171	4420	5400	0.02	0.003	0.618	0.004	39.4	10.1	0.32	0.025	6.2
P3	4.1	170	3180	2000	0.02	bdl	0.479	bdl	23.1	7.8	0.26	bdl	0.1
Detection limits													
					0.002	0.002	0.002	0.002	0.01	0.002	0.005	0.005	0.002
Reproducibility (%)													
	±0.03			±5.25	±0.02	±0.002	±0.006	±0.0007	±2.21	±0.01	±0.07	±0.007	±0.04

bdl: below detection limit
Silver, Hg and Sb below detection limit for all samples analyzed
Sample coordinates:
P1: N40°53´47.1˝ E25°37´44.8˝
P2: N40°54´43.9˝ E25°38´02.8˝
P3: N40°54´10.0˝ E25°37´31.0˝

The mineralogy of samples studied by SEM, XRD and optical microscopy studies revealed that the physicochemical environment, related to the lower sulfide sector, changes rapidly at the transition zone between the andesitic breccia and the overlying sandstone. Secondary, supergene phases are present indicating that supergene alteration phenomena have affected the disseminated ore hosted in the felsic sandstone. Mineralogical studies of drill core samples reveal that the lower limit of the oxidation zone roughly follows the boundary between the andesitic breccia and the sandstone and reaches approximately 100 m at depth at the center (90 m for borehole Pd10, Fig. 2), whereas is limited at the sides of the deposit ranging from 20 to 25 m from the surface (Fig. 1C) (Skarpelis et al., 2006; Triantafyllidis, 2006).

Pervasive oxidation is identified in near surface samples with a maximum depth of 45 to 50 m at the center (Fig. 2). Liesegang bands, scarce remnants of pyrite and tennantite, significant load in secondary goethite and hematite as impregnations with fine-grained kaolinite (Fig. 3B) and disseminated native Au

(Skarpelis et al., 2006) characterize the upper, extensively leached and oxidized part of the deposit. Highly insoluble anglesite replacing galena is the only supergene phase observed in the upper part of the oxide sector. At the lower levels of the Perama sandstone and up to the transition zone with the underlying andesitic breccia, supergene alteration phenomena are less extensive (Fig. 2). Goethite and hematite are present in fractures and fissures of the silicified sandstone, but also as aggregates and patches with kaolinite. Pyrite is locally replaced by jarosite (Fig. 3E).

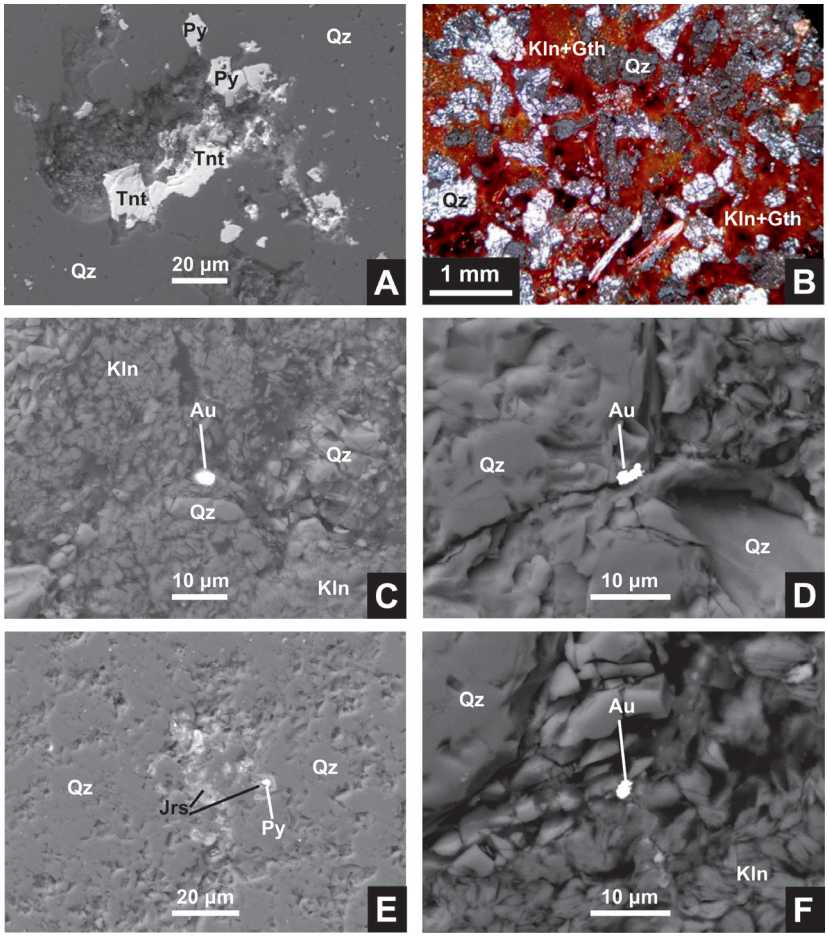

Fig. 3. *A. Tennantite in association with pyrite in the sulfide sector. B. Impregnations of goethite and hematite in kaolinite patches between angular-subangular quartz clasts in the upper, pervasively altered part of the oxide sector. C. Free Au grains from the upper part of the oxide sector. D. Free Au grain from the lower part of the oxide sector. E. Pyrite alteration to jarosite at the lower level of the oxide sector. F. Free Au grains from the lower part of the oxide sector near the transition zone.*

Εικ. 3. *Α. Τενναντίτης σε επαφή με σιδηροπυρίτη στο πυριτιωμένο ανδεσιτικό breccia. Β. Εμποτισμοί γκαιτίτη και αιματίτη σε μάζες καολινίτη μεταξύ γωνιώδων-υπογωνιώδων κλαστών χαλαζία από το ανώτερο, έντονα εξαλλοιωμένο τμήμα του ψαμμίτη. C. Κόκκοι Au από το ανώτερο τμήμα του ψαμμίτη του Περάματος. D. Κόκκοι Au από το κατώτερο τμήμα του ψαμμίτη. Ε. Οξείδωση σιδηροπυρίτη προς γιαροσίτη στο κατώτερο τμήμα του ψαμμίτη. F. Κόκκοι Au από το κατώτερο τμήμα του ψαμμίτη του Περάματος κοντά στη ζώνη μετάβασης.*

Supergene alteration phenomena are active as it is proved by the quality of surface and ground water samples collected in the vicinity of the Perama Hill deposit. All samples fall into the quality range of waters draining several epithermal deposits globally (Koyanagi and Panteleyev, 1993; Plumlee et al., 1995; Skarpelis and Triantafyllidis, 2004). In particular, the drainage waters are characterized by increased Fe, Mn and Ni content and very low concentrations of Cu, Pb and As, whereas the Fe content decreases along with distance distance to the ore deposit (Tabl. 4). The surface and ground water samples collected in the vicinity of the Perama Hill deposit are characterized as acidic to extreme acidic with high metal load when plotted on a Ficklin diagram with pH values less than 5.5 and total heavy metal load higher than 1mg/L (Triantafyllidis, 2006).

4.3. Native Gold

Optical microscopy and SEM studies proved that native Au grains, with ranging Ag content, are present in the oxide sector of the Perama Hill epithermal deposit. Free Au predominates in the upper (depth up to 10m from the surface) and the lowermost part of the Perama sandstone, near the transition zone between the sandstone and the sulfidic ore. That observation is in line with Juras et al. (2010) who state that the highest gold grades are identified in drill core samples from the upper and the lower part of the oxide sector. In the oxide sector, native Au is either associated with Kaolinite and goethite, or it appears between quazz clasts with size ranging between 1 to 10μm (Figs 3C, 3D, 3F). On the other hand, mineralogical investigation of samples from the sulfide sector revealed no free Au grains.

5. Discussion

The distribution of secondary phases in the oxide sector provides insights on the physicochemical conditions and the maturity of the physicochemical environment of both the upper and the lower part of the deposit. Secondary Fe(III) phases goethite and hematite prevail in the upper part, whereas jarosite and other Fe-sulfates are present at lower levels (Fig. 2). According to Walton-Day (1999), Newbrough and Gammons (2002), Courtin-Nomade et al. (2003), and Fukushi et al. (2003) typical secondary phases in oxidation zones resulting from alteration of Fe-sulfides and sulfosalts include ferrihydrite, schwertmannite, jarosite, goethite and hematite. The stability of those minerals depends on the prevailing physicochemical conditions with increasing pH and decreasing sulfate load the series of replacement is as follows:

Jarosite → schwertmannite → ferrihydrite → goethite → hematite

Goethite and hematite are the most stable secondary Fe(III) phases in mildly acidic to alkaline and oxidative conditions (Nordstrom and Alpers, 1999). It is therefore reasonable to assume that as supergene alteration phenomena progressed, the geochemical environment of the upper part of the oxide sector gradually changed from highly oxidative with increased sulfate load, to mildly acidic and oxidative with very low sulfate content. This pervasive oxidation of the ore is enhanced in the central part of the deposit reaching depths to 45m (Fig. 2). The presence of goethite and hematite combined with the absence of secondary sulfates (e.g. jarosite), and the depletion of most heavy metals, based on the geochemical profiles of

the bore-holes studied, indicate a mature physicochemical environment and progressively increasing pH and decreasing sulfate load. Liesegang bands also support the hypothesis of mature physicochemical conditions and limited advent flow, since the characteristic rings result from diffusion of oxygen with Fe-rich fluids in poorly lithified sediments (Balsamo et al., 2013; Stegena, 1983). The hypothesis on mature environment is also supported by the enrichment of goethite in As in near-surface samples. In slightly acidic to neutral conditions the concentration of soluble As is controlled by the presence of Fe oxides/hydroxides. Secondary Fe(III) phases show positive surface charge enabling adsorption of negatively charged anions and oxyanions of As (Smith, 1999; Sracek et al., 2004) with maximum adsorption in pH between 3 and 5 (Garcia-Sanchez and Alvarez-Ayuso, 2003).

During the early stages of supergene alteration, the mineralogy of the host sandstone combined with the disseminated mode of occurrence of hypogene minerals and the high potential of pyrite and tennantite to produce highly oxidative agents (Plumlee, 1999), enhanced oxidation phenomena resulting in liberation of microparticulate Au. In oxidative near-surface environments of sulfide deposits two major mechanisms of Au solubility exist, metastable thiosulfate (Webster, 1986; Renders and Seward, 1989) and chloride complexes (Mann, 1984; Webster and Mann, 1984; Stoffregen, 1986), where the Ag content of free Au may provide insights on the prevailing geochemical conditions. In the presence of chlorides, Ag is more readily dissolved relative to Au (Craw et al., 2015) resulting in Au grains with very low Ag content. Scanning Electron Microscopy study revealed that free Au grains in the oxide sector of the Perama deposit show a ranging Ag content (between 1 and 3 wt%) indicating co-deposition of Au with Ag. It means that thiosulphate-mediated dissolution of Au was most likely the major Au transport mechanism in early stages of supergene alteration. During the evolution of the upper part of the oxide sector of the Perama Hill deposit, the physicochemical environment changed from acidic and oxidative, to mature (near-neutral and oxidative). In such conditions, Au is highly insoluble and is mainly transported as elemental, colloidal Au (Krauskopf, 1951), favoring small scale migration, aggregation and re-deposition as free Au grains (Fig. 3C, 3F).

At the lower levels of the oxide sector, the oxidation phenomena are still active but not pervasive. This view is supported by the varying degree of alteration of hypogene sulfides and sulfosalts. In several occasions pseudomorphs of goethite after pyrite and jarosite grains around pyrite crystals are observed (Fig. 3E). The presence of secondary Fe-sulfates indicates relatively immature environment, oxidative conditions and increased sulfate load (Walton-Day, 1999; Courtin-Nomade et al., 2003), an hypothesis supported by the acidic nature and the high metal load of surface and groundwaters draining the Perama sandstone (Tabl. 4). Meteoric waters penetrate the porous sandstone and still attack the disseminated ore comprising pyrite and tennantite resulting in very low quality drainage. It seems that the geochemical environment of the lower part resembles the conditions of the near-surface sector of the deposit during the early stages of supergene alteration. Oxidative, rich in sulfates fluids resulting from on-going oxidation of

sulfides and sulfosalts favor solubility of Au as thiosulfate complexes. As physicochemical conditions change near the transition zone between the oxide and the sulfide sector of the deposit, aggregation and reprecipitation of native Au grains among quartz clasts occurs (Fig. 3D), resulting in enrichment of the lower part of the oxide sector in gold (Fig. 2).

The mode of occurrence of Au in the oxide sector of the Perama Hill deposit is a combination of detrital, later hydrothermal and subsequent supergene alteration mineralogy. The Perama sandstone is characterized by uniform mineral assemblage with abundant quartz, kaolinite, minor illite and traces of K-feldspar. As stated by Lescuyer et al. (2003), the Perama sandstone contains angular to subangular fragments of the basement metamorphic rocks (quartz grains and polycrystalline quartz clasts and mica), as well as glass shards and pyroclastic fragments related to felsic eruptions of the Petrota graben. The immature, felsic sandstone is characterized by increased porosity (coarse, angular to subangular clasts, Fig. 3B). That porosity played a very important role when the sandstone was later affected by hydrothermal activity related to the original high sulfidation mineralogy and the final development of the intermediate sulfidation system. Acidic hydrothermal fluids followed feeders and conduits, and also diffused in the porous media, resulting in extensive hypogene alteration of detrital feldspars and micas to fine-grained kaolinite that filled voids and cracks in the Perama sandstone, providing the final assemblage with very low acid buffering capacity. Uplift and subsequent supergene alteration resulted in oxidation of hypogene disseminated sulfides and sulfosalts, liberation of microparticulate Au, migration, aggregation and deposition of free Au grains.

6. Conclusions

Extensive supergene alteration phenomena have affected the upper part of the Perama Hill epithermal mineralization hosted in the felsic sandstone, whereas oxidation is very limited at the lower sulfide sector. It seems that rock heterogeneity between the underlying andesitic breccia and the overlying porous sandstone played a critical role in development of the texture of the mineralization and the following geologic evolution. The disseminated nature of the ore, with pyrite being the predominant sulfide, combined with the texture and limited acid-buffering capacity of the host sandstone favored penetration of slightly acidic and oxidative meteoric waters and subsequent oxidation phenomena. Goethite and hematite predominate at the uppermost part of the deposit, whereas secondary phases of other heavy metals occur as minor constituents (e.g. anglesite), or are lacking (e.g. Cu and Zn) revealing pervasive supergene oxidation and leaching. At lower levels secondary Fe sulfates are identified, indicating locally highly acidic and oxidative conditions and immature geochemical environment. Free Au grains are observed in the upper and lowermost part of the oxide sector of the deposit, observation that is in line with statements by Juras et al. (2010). Oxidation phenomena still affect the disseminated ore and enrich the ore in free Au near the transition zone between the underlying andesitic breccia and the overlying sandstone. Supergene alteration phenomena are active till this day as proved by the acidic and oxidative and rich in heavy metals, surface and ground drainage at the Perama sandstone.

Acknowledgements
Part of the research work was funded through the program "IRAKLEITOS – Fellowships for Research of National and Kapodistrian University of Athens – ENVIRONMENT". We thank Prof. M. Vavelidis and Ass. Prof. St. Kalaitzidis for their constructive reviews.

References

Balsamo, F., Bezzera, F.H.R., Vieira, M.M. Storti, F., 2013. Structural control on the formation of iron-oxide concretions and Liesegang bands in faulted, poorly lithified Cenozoic sandstones of the Paraíba Basin, Brazil. *Bulletin of GSA*, 125, 5-6, 913-931.

Border, A.L.M., Michael, C., Constantinides, D., 1999. Discovery and evaluation of the Sappes gold deposits, NE Greece. *New Generation GOLD 99*, Perth, Western Australia.

Bridges, P. S., Gordon, M. J., Michael, C., Abatzioglou, M., 1997. Gold mineralization at Sappes, Northern Greece. *Irish Association for Economic Geology Ltd*, 95-107.

Christofides, G., Soldatos, T., Eleftheriadis, G., Koroneos, A., 1998. Chemical and isotopic evidence for source contamination and crustal assimilation in the Hellenic Rhodope plutonic rocks. *Acta Vulcanologica*, 10, 305-318.

Courtin-Nomade, A., Bril, H., Neel, C., Lenain, J-F., 2003. Arsenic in iron cements developed within tailings of a former metalliferous mine-Enguiales, Aveyron, France. *Applied Geochemistry*, 18, 9, 395-408.

Craw,D., MacKenzie, D., Grieve, P., 2015. Supergene gold mobility in orogenic gold deposits, Otago Schist, New Zealand. *New Zealand Journal of Geology and Geophysics* (DOI: 10.1080/00288306.2014.997746).

Dill, H.G., 2001. The geology of aluminium phosphates and sulphates of the alunite group minerals: a review. *Earth-Science Reviews*, 53, 35-93.

Eleftheriadis, G., 1990. Petrology and geochemistry of the Oligocene volcanic rocks from the Central Rhodope Massif (N. Greece). *Geol. Rhodopica*, 2, 180-196.

Fukushi, K., Sasaki, M., Sato, T., Yanase, N., Amano, H., Ikeda, H., 2003. A natural attenuation of arsenic in drainage from an abandoned arsenic mine dump. *Applied Geochemistry*, 18, 9, 1267-1278.

Garcia-Sanchez, A., Alvarez-Ayuso, E., 2003. Arsenic in soils and waters and its relation to geology and mining activities (Salamanca Province, Spain). *Journal of Geochemical Exploration*, 80, 69-79.

Jambor, J.L., 1999. Nomenclature of the alunite supergroup. *Canadian Mineralogist*, 37, 1323-1341.

Juras, S., Miller, R., Perkins, P., 2010. Technical Report, of the Perama Hill Project, Thrace, Greece. Unpublished Report, Eldorado Gold Corporation, 144p.

Koyanagi, V.M., Panteleyev, A., 1993. Natural acid drainage in the Mount Macintosh/Pemberton Hills area, northern Vancouver Island (92L/12), in: Grant, B. et al. (Eds), *Geological fieldwork 1992 - a summary of field activities and current research*: Ministry of Energy, mInes, and Petroleum Resources, Report 1993-1, 445-450.

Krauskopf, K.B., 1951. The solubility of gold. *Econ. Geol*. 46, 858–870.

Krohe, A., Mposkos, E., 2002. Multiple generations of extensional detachments in the Rhodope Mountains (northern Greece): evidence of epi-

sodic exhumation of high-pressure rocks, in: Blundell, D.J., Neubauer, F., VonQuadt, A., (Eds.), *The Timing and Location of Major Ore Deposits in an Evolving Orogen*. Geological Society, London, Special Publication, 204, 151-178.

Lescuyer, J.L., Baily, L., Cassard, D., Lips, A.L.W., Piantone, P., McAlister, M., 2003. Sediment-hosted gold in south-eastern Europe: the epithermal deposit of Perama, Thrace, Greece. *7th Biennial SGA Meeting, Mineral Exploration and Sustainable Development*, Athens, 499-502.

Mann, A.W., 1984. Mobility of gold and silver in lateritic weathering profiles; some observations from Australia. *Econ. Geol*., 79, 38–49.

Marschik, R., Schmidt, E., Falalakis, G., Hölzl, S., 2011. The Perama Hill gold deposit, NE Greece: Strontium, lead, and sulfur isotope signature of the hypogene mineralization, in: Barra F. et al. (Eds) *Let's Talk Ore Deposits*, 11th Biennial SGA Meeting of The Society for Geology Applied to Mineral Deposits, Antofagasta, Chile, 496-498.

McAlister, M., Hammond, M.J., Normand, D., Kampasalakis, M., 1999. Discovery case history for the Perama Hill Gold deposit, Greece, in: Currie, D., Nielsen, K., (Eds). *New Generation Gold Mines 99*, Case Histories of Discovery, Perth, Australia, 39-49.

Michael, C., Constantinides, D., Ashworth, K., Perdikatsis, V., Demetriades, A., 1989. The Kirki vein polymetallic mineralization, NE Greece. *Geologica Rhodopica*, 1, 366-373.

Michael, C., Papadopoulos, P., Marantos, I., Evangelou, E., 1988. Epithermal gold mineralization in Konos area, Institite of Geology and Mineral Exploration, Athens, [in Greek]. 23p.

Michael, C., Perdikatsis, V., Dimou, E., Marantos, I., 1995. Hydrothermal alteration and ore deposition in epithermal precious metal deposit of Agios Demetrios, Konos area, northern Greece. *Geol. Soc. Greece*, Special Publication, 4, 2, 778-782.

Newbrough, P., Gammons, C.H., 2002. An experimental study of water-rock interaction on acid rock drainage in the Butte mining district, Montana. *Environmental Geology,* 41, 705-719.

Nordstrom, D.K., Alpers, C.N., 1999. Geochemistry of acid mine waters, in: Plumlee, G.S., Logsdon, M.J., (Eds.), Reviews in Economic Geology, 6A. *The Environmental Geochemistry of Mineral Deposits. Part A: Processes, Techniques, and Health Issues*, Society of Economic Geologists, 133-160.

Pecskay, Z., Eleftheriadis, G., Koroneos, A., Soldatos, T., Christofides, G., 2003. K/Ar dating, geochemistry and evolution of the tertiary volcanic rocks (Thrace, Northeastern Greece). *7th Biennial SGA Meeting, Mineral Exploration and Sustainable Development*, Athens, 1229-1232.

Plumlee, G.S., 1999. The environmental geology of mineral deposits, in: Plumlee, G.S., Logsdon, M.J., (Eds.), Reviews in Economic Geology, 6A. *The Environmental Geochemistry of Mineral Deposits, Part A: Processes, Techniques, and Health Issues*, Society of Economic Geologists, 71-116.

Plumlee, G.S., Smith, K.S., Mosier, E.L., Ficklin, W.H., Montour, M., Briggs, P.H., Meier, A.L., 1995. Geochemical processes controlling acid-drainage generation and cyanide degradation at Summitville, in: Posey, H.H., Pendleton, J.A., VanZyl, D., (Eds.), *Sum-*

mitville Forum, Colorado Geological Survey Spec. Pub. 38, 23-34.

Renders, P.J.N., Seward, T.M., 1989. The stability of hydrosulphido- and sulphido-complexes of Ag (I) and Au (I) at 25 ºC. *Geochim. Cosmochim. Acta*, 53, 245-253.

Scott, K.M., 1987. Solid solution in and classification of gossan-derived members of the alunite jarosite family, Northwest Queensland, Australia. *American Mineralogist*, 72, 178-187.

Shaw, A.J., Constantinides, D.C., 2001. The Sappes gold project. In: Marinos et al. (Eds.), *9th Inter. Congr. Geol. Soc. Greece*, Athens, 1073-1080.

Smith, K.S., 1999. Metal sorption on mineral surfaces: an overview with examples relating to mineral deposits, in: Plumlee, G.S., Logsdon, M.J., (Eds.), Reviews in Economic Geology, 6A. *The Environmental Geochemistry of Mineral Deposits. Part A: Processes, Techniques, and Health Issues*, Society of Economic Geologists, 161-182.

Skarpelis, N., Triantafyllidis, S., 2004. Environmental impact form supergene alteration and exploitation of a high sulphidation epithermal type mineralisation (Kirki, NE Greece). *Applied Earth Science, Trans. Inst. Min. Metall. B*, 113, 1, 110-116.

Skarpelis, N., Economou, M., Michael, K., 1987. Geology, petrology and polymetallic ore types in a Tertiary volcanosedimentary terrain, Virini-Pessani-Dadia area, West Thrace (Northern Greece). *Geologica Balcanica*, 17, 6, 31-41.

Skarpelis, N., Triantafyllidis, S., Falalakis, G., 2006. The Perama intermediate sulfidation epithermal Au system (Thrace, Greece): Hypogene mineralogy and supergene alteration. *Neogene Magmatism of the Central Aegean and Adjacent Areas: Petrology, Tectonics, Geodynamics, Mineral Resources and Environment*, Milos, Cyclades, Greece, abstracts vol., p37.

Skarpelis, N., Voudouris, P., Arikas, K., 1999. Exploration for epithermal Gold in SW Thrace (Greece): New target areas, in Stanley, C.J. et al. (Eds.) *Mineral Deposits: Processes to Processing*, Rotterdam: Balkema, 589-592.

Sracek, O., Bhattacharya, P., Jacks, G., Gustafsson, J-P., VonBromssen, M., 2004. Behavior of arsenic and geochemical modeling of arsenic enrichment in aqueous environments. *Applied Geochemistry*, 19, 169-180.

Stegena, L., 1983. Leaching in rocks: some physical principles, in: Augustithis, S.S., (Eds.), *Leaching and diffusion in rocks and their weathering products*, Theophrastus Publications, Athens, Greece, 81-92pp.

Stoffregen, R., 1986. Observations on the behavior of gold during supergene oxidation at Summitville, Colorado, USA, and implications for electrum stability in the weathering environment. *Applied Geochemistry,* 1, 549–558.

Struntz, H., Tennyson, C., 1982. Mineralogische Tabellen. Akademische Verlagsgesellschaft Geest and Portig, Leipzig, 621p.

Triantafyllidis, S., 2006. *Environmental risk assessment of mining and processing activities and rehabilitation proposals in Evros and Rhodope prefectures* (Thrace, NE Greece). Unpublished PhD Thesis (in Greek with English abstract), Faculty of Geology & Geoenvironment, University of Athens, 361p.

Voudouris, P., Melfos, V., Vavelidis,

M., Arikas, K., 2003. Genetic relation between the Tertiary porphyry Cu-(±Mo) and the epithermal Au-(±Ag) deposits in the Rhodope metallogenic province, Thrace region, Northern Greece. *7th Biennial SGA Meeting, Mineral Exploration and Sustainable Development*, Athens, 541-544.

Voudouris, P., Papavassiliou, C., Alfieris, D., Falalakis, G., 2007. Gold-silver tellurides and bismuth sulfosalts in the high-intermediate sulfidation Perama Hill deposit, western Thrace (NE Greece). *Geological Survey of Finland*, Guide 53, 77-84.

Walton-Day, K., 1999. Geochemistry and processes that attenuate acid mine drainage in wetlands, in: Plumlee, G.S., Logsdon, M.J., (Eds.), Reviews in Economic Geology, 6A. *The Environmental Geochemistry of Mineral Deposits. Part A: Processes, Techniques, and Health Issues*, Society of Economic Geologists, 215-228.

Webster, J.G., 1986. The solubility of gold and silver in the system Au–Ag –S–O2–H2O at 25 ºC and 1 atm. *Geochim. Cosmochim. Acta*, 50, 1837-1845.

Webster, J.G., Mann, A.W., 1984. The influence of climate, geomorphology and primary geology on the supergene migration of Au and Ag. *Journal of Geochemical Exploration*, 22, 21–42.

Whitney, D.L., Evans, B. W., 2010. Abbreviations for names of rock-forming minerals. *American Mineralogist, 95*, 185-187.